Localization of HIV RNA in Mitochondria of Infected Cells: Potential Role in Cytopathogenicity

Mohan Somasundaran, Maria L. Zapp,* Lars K. Beattie,‡ Lizhen Pang,‡ Kevin S. Byron, Gary J. Bassell,‡ John L. Sullivan, and Robert H. Singer‡

Program in Molecular Medicine and Departments of Pediatrics,* Biochemistry, and ‡Cell Biology, University of Massachusetts Medical Center, Worcester, Massachusetts, 01605

Abstract. The intracellular distribution of HIV-1 RNA transcripts in infected cells was studied using in situ hybridization detected by electron microscopy and cellular fractionation. Although viral RNA and core protein could be detected throughout the cytoplasm and nucleus, viral RNA was found in significantly increased amounts in mitochondria relative to the cytoplasm and nucleus. In contrast, cellular poly(A) RNA or viral *gag* proteins were not increased in the mitochondria. A cell line containing an integrated latent genome that could be induced to express viral RNA after phorbol ester stimulation showed an increase in viral RNA accumulation in mitochondria parallel with the increase in HIV expression levels. Concomitant with HIV expression, there was a decrease in mitochondrial viability. Using immunofluorescent markers to detect probes to HIV RNA transcripts and antibodies to mitochondrial proteins simultaneously in single cells, there was an inverse relationship between the amount of viral RNA and mitochondrial integrity. High levels of viral RNA in mitochondria were found in acutely (but not chronically) infected cells. We propose that HIV RNA import into mitochondria can compromise mitochondrial function.

It is now accepted that HIV-1 infection of CD4 T lymphocytes results in a cytopathic effect; however, it is not known how this effect is mediated. A number of hypotheses have been suggested to explain HIV-1–induced CD4 T cell lysis. Fusion of infected cells with uninfected cells (syncytium formation) was suggested as a mechanism for cell death and depletion of CD4 T cells in vivo (15, 28). Accumulation of extrachromosomal HIV DNA in infected cells has also been associated with cell death (19, 21). Several investigators have suggested that HIV infection induces programmed cell death or apoptosis and leads to CD4 depletion in vivo (12, 31). Intracellular HIV-gp160/120 and CD4 complex formation (9, 11) and cytokine-mediated cell death (17, 22) have also been implicated in HIV-induced cytopathogenicity.

We have investigated the hypothesis that there is a direct cytolytic effect of HIV RNA (genomic or mRNA transcripts) on the infected cell. The dramatic loss of CD4 T cells over time after HIV infection may be directly mediated by the virus and not secondarily by syncytium-formation or apoptosis. Earlier observations suggested that HIV infection resulted in cytotoxic effects on individual infected cells in culture (single-cell killing) via a mechanism involving high viral load (29, 30). Since then, it has been observed that high quantities of virus are associated with HIV infection in vivo (8, 20, 23). The intracellular distribution of HIV transcripts has been studied directly using in situ hybridization. In chronic or acute infection, viral RNA is apparent in the nucleus as a primary focus representing the site of transcription, as well as dispersed throughout the cytoplasm (13). Viral RNA signals in acute productive infection become intense in the cytoplasm later in infection, before cell lysis. In stable producer cell lines, the chronic level of infection results in a cytoplasmic signal that is much less. This suggests a relationship between cytopathogenecity and viral RNA levels in the cytoplasm.

Since viral protein synthesis and virion formation occur at sites of HIV RNA accumulation, a high resolution approach to intracellular localization of HIV-1 RNA may reveal the cellular sites where the cytopathic effect is manifested. Concentration of viral RNA within or around specific cellular organelles may give insights into the mechanism. To achieve high resolution localization of viral RNA, in situ hybridization was combined with detection by electron microscopy (1). Results from this approach showed that high concentrations of viral RNA were found preferentially in mitochondria relative to the cytoplasm and nucleus. In contrast, neither viral core protein nor poly(A) RNA was increased in the mitochondria. Using an inducible cell line (6), HIV RNA was observed to traffic into mitochondria within a short time. Import of RNA into mitochondria would be expected to result from *cis*-acting sequences in HIV RNA, perhaps in

Address all correspondence to Mohan Somasundaran, Department of Pediatrics, Program in Molecular Medicine, University of Massachusetts Medical Center, Two Biotech, 373 Plantation Street, Worcester, MA 01605.

combination with cellular factors. Such a model exists in nucleo-mitochondrial pathways for the RNA component of the mitochondrial RNA processing (MRP)[1] endonuclease in yeast and mice (2, 14). Import of this RNA into mitochondria requires *cis*-acting sequences (14). The accumulation of viral RNA in mitochondria would be expected to be deleterious to this organelle. In support of this, a decrease in mitochondrial viability was observed concomitant with the increase in viral RNA in mitochondria. These results suggested that this mitochondrial concentration of HIV may play a role in the cytopathic effect of the virus.

Materials and Methods

Mitochondrial Fractionation and Northern Analyses

Mitochondrial fractions were prepared using a modification of the procedure described by Topper et al. (32). Briefly, uninfected A3.01 cells and chronically infected HIV-positive ACH2 cells were stimulated with 12-*O*-tetradecanoyl-phorbol-13-acetate (TPA) for 6 h. Before fractionation, cells were pretreated with RPMI medium containing 10% fetal calf serum, 200 μg/ml puromycin (to dissociate polysomes), and 10 μg/ml cytochalasin (to disrupt actin filaments) for 15 min at 37°C. All subsequent steps were performed at 4°C. Cells were washed once in PBS and resuspended in reticulocyte standard buffer (10 mM Tris-HCl, pH 7.5; 10 mM NaCl; 1.5 mM $CaCl_2$; 4 mM vanadyl ribonucleoside complex) to swell for 15 min. Cells were disrupted with a Dounce homogenizer, and an equal volume of 2× mitochondrial standard buffer was added to obtain a final concentration of 1× buffer (5 mM Tris-HCl, pH 7.5; 210 mM mannitol; 70 mM sucrose; 5 mM EDTA; 4 mM vanadyl ribonucleoside complex). Nuclei and undisrupted cells were removed by three sequential centrifugations at 1,500 *g* for 5 min. The supernatant was then centrifuged at 8,000 *g* for 10 min to obtain a mitochondria-enriched pellet and a cytoplasm-enriched supernatant. The pellet was analyzed for mitochondrial purity by standard electron microscopy. RNA was extracted from unfractionated A3.01 cells, ACH2 cells, and the mitochondria-enriched pellet, and cytoplasm-enriched fraction using guanidinium thiocyanate/phenol method (33).

To purify the mitochondria further, the mitochondria-enriched pellet was also subjected to Nycodenz gradient analysis. The pellet was resuspended in sucrose-TE buffer (5 mM Tris-HCl, pH 7.5; 250 mM sucrose; 1 mM EDTA). This suspension was loaded onto 20–40% Nycodenz gradient and centrifuged at 140,000 *g* for 90 min. A total of 13 fractions (100 μl each) were collected and RNA was extracted from each fraction (33). Each fraction was analyzed by Northern analysis with consecutive 12S rRNA (mitochondria) probe and HIV probe hybridizations, and the counts per min from the bands in each lane quantitated by a Beta-scope blot analyzer (Beta-Gen, Mountain View, CA).

Northern analyses were performed according to standard protocol. HIV RNA, 12S mitochondrial rRNA and U1 snRNA were analyzed on the same RNA blot. HIV-RNA was detected with a ^{32}P-labeled RNA probe that hybridized to spliced and unspliced HIV messages and was complementary to the U3 region of HIV-long terminal repeats (30). The probe to 12S mitochondrial rRNA was a oligonucleotide (40mer), 5′ end-labeled with ^{32}P. Polymerase chain reaction was used to synthesize [^{32}P]dCTP incorporated U1 snRNA probe.

In Situ Hybridization and Electron Microscopic Analyses

In situ hybridization was performed on HIV-infected cells by the method described earlier (26, 27). The full-length (8.9 kb) pHXB-2 HIV DNA (25) was biotinylated by nick translation and was used to detect viral RNA. For detection, a primary rabbit-antibiotin polyclonal antibody (Enzo Biochem Inc., New York) (1 h, 37°C) and a secondary goat-anti-rabbit-IgGl-1 nm-Au-conjugated antibody (Amersham Corp., Arlington Heights, IL) (2 h, 37°C) were suspended in BTSSC (1× SSC, 1% BSA Fraction V [Sigma Immunochemicals, St. Louis, MO], 1% Triton X-100 [Boehringer Mannheim GmbH, Mannheim, Germany]) and added to the cells. After antibody incubations, the cells were washed with 1× SSC three times (3 min each). The 1 nm-Au particles bound to the HIV-1 DNA probe were then silver enhanced (Amersham Corp.). Enhancements were monitored on a light microscope and stopped when sufficient signal was obtained (usually 7–10 min). The enhancement solution was washed off the cells in water briefly, and the cells were dehydrated stepwise in ethanol. Once dehydrated, the cells were embedded in epon, sectioned, and stained using standard techniques. The variation in sizes of mitochondria observed in the panels were caused by random sectioning of cells that resulted in longitudinal or transverse sections of mitochondria.

To detect HIV RNA directly in thin sections of cells, cells were embedded in LR White (5) and viral RNA were detected directly with a novel technique using oligonucleotide probes. 20 biotinylated oligonucleotide probes (35 mers, five biotins coupled per oligonucleotide) specific to the *gag*, *pol*, and *env* regions of HTLV-IIIb (3 ng/μl probe, 60 ng/μl competitor oligonucleotides, 50% formamide, 5% dextran sulfate, 2× SSC, 20 μl total volume) were incubated on LR White sections of cells at 37°C for 1 h in a moist chamber. After washing the probe in 50% formamide, 2× SSC once and twice in 2× SSC (20 "dips" each), a primary rabbit-antibiotin polyclonal antibody (Enzo Biochem Inc.) (1:100 dilution), and a secondary goat-anti-rabbit-IgGl-6 nm-Au-conjugated antibody (Jackson Immunoresearch Laboratories, Inc., West Grove, PA) were used to detect the hybridized oligonucleotides. Antibodies were suspended in BTSSC (1× SSC, 1% BSA Fraction V [Sigma Immunochemicals], 1% Triton X-100 [Boehringer Mannheim GmbH]), and washed off in 1× SSC. Afterwards, the sections were stained using concentrated uranyl acetate and Reynold's lead citrate.

Quantitative and Statistical Analyses of Signals (HIV RNA) in Electron Micrographs

Cells were exposed to appropriate reagents and HIV-1 RNA or *gag* proteins detected as described above. Random cells were photographed in the electron microscope after sectioning. The photographs of 10 random cells from each of several experiments were analyzed under high magnification, and the silver grains in cytoplasm (minus mitochondria) and the mitochondria were quantitated after digitizing the prints using a solid-state charge-coupled device camera (Cohu, San Diego, CA). The analyses were done using a morphometric computing software (Imagemeasure; Microscience Inc., Seattle, WA) along with an interactive screen (Werner Frey, Image Lab, Santa Monica, CA) and an Equity II computer (Epson America, Inc., Torrance, CA). Grains were counted manually within each area outlined for the computer. Area (in square microns) were computed using internal markers and the magnification of the print. The percentage of silver grains within mitochondria and the percentage of silver grains outside mitochondria were calculated. The density of grains was determined as the percentage of grains divided by the percentage of the area. The $\log_{10}$ of these values were determined to be normalized by skew and Kurtosis analyses. A Student's *t* test was performed on these numbers to determine statistical significance (*P* value) of (*a*) the localization of viral RNA in mitochondria, and (*b*) increased levels of viral RNA in mitochondria of acutely infected cells. Note that when counting random cells from acutely infected cultures, some cells vary in their levels of viral expression, causing an average that is less than that found in highly infected cells. ACH2 cells were induced by the phorbol ester, TPA, and samples were taken at various times. Cells were analyzed for mitochondrial accumulation of signal using the methods described above.

Fluorescent In Situ Hybridization Analyses

ACH2 cells were stimulated with TPA for 6 h, washed twice in PBS, and air dried on gelatin-coated slides. After fixation in 4% paraformaldehyde, the cells were washed and HIV RNA was detected by a fluorescent in situ hybridization technique using biotinylated HIV-specific probes and avidin-FITC as secondary reagent according to previously described procedures (26, 27). A monoclonal antibody specific to a 65-kD mitochondrial structural protein (Chemicon International, Temecula, CA) was used to stain mitochondria and goat anti-mouse IgG-TRITC was used as secondary reagent to detect mitochondria.

Viability Assay for Mitochondria (MTT Assay)

A fixed number (40,000) of TPA-induced ACH2 and A3.01 cells from each time-point were monitored for viable mitochondria using a colorimetric assay described by Denizot and Lang (3). The optical density of reduced methyl thiazolyl tetrazolium (MTT) dye was measured at 570 nm and is equivalent to the activity of dehydrogenase associated with active mitochon-

1. *Abbreviations used in this paper*: MRP, mitochondrial RNA processing; MTT, methyl thiazolyl tetrazolium; TPA, 12-*O*-tetradecanoyl-phorbol-13-acetate.

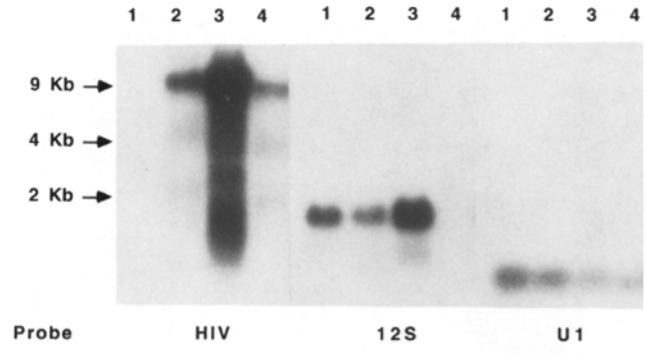

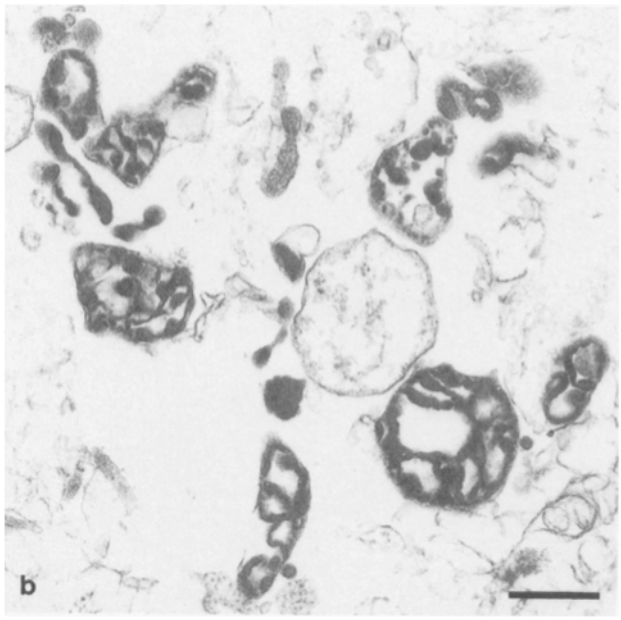

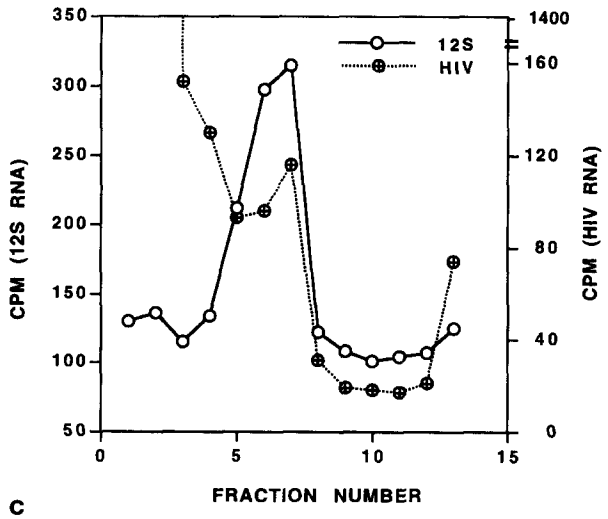

Figure 1. Detection of HIV-1 RNA in cytosolic fractions of infected cells. Subcellular fractionation and Northern analyses are described in Materials and Methods. (*a*) Mitochondrial 12S rRNA, HIV RNA, and U1 snRNA were detected by successive Northern analyses. Each lane was loaded with 12.3 μg of RNA. Lane *1*, total cellular RNA from uninfected A3.01 cells (1% of total); lane *2*, total cellular RNA from TPA-stimulated ACH2 cells (1% of total); lane *3*, RNA from mitochondria-enriched pellet of TPA-stimulated ACH2 cells (100% of the pellet); lane *4*, RNA from cytoplasmic supernatant of TPA-stimulated ACH2 cells (1% of total). (*b*) Electron micrograph of the mitochondria-enriched pellet. Bar, 0.5 μm. (*c*) Comigration of mitochondria (12S rRNA) and HIV RNA by Nycodenz sedimentation velocity centrifugation. Fractions were extracted, electrophoresed, blotted, and probed for 12S rRNA and HIV RNA successively. The ^{32}P radioactivity in each lane was measured by Beta-scope analysis instrument and expressed as counts per minute.

dria. At the same time, density of viral RNA in mitochondria was determined as described above.

Results and Discussion

HIV RNA Transcripts in Mitochondria

Previous reports have suggested a role for mitochondria in retroviral replication (4, 7, 10). To investigate the intracellular distribution of HIV RNA (a member of *lentivirus* family of retroviruses), a mitochondria-enriched pellet and cytoplasm-enriched supernatant were prepared from TPA-induced ACH2 cells and were analyzed for HIV RNA. Northern blot analysis demonstrated the presence of HIV RNA in the mitochondria-enriched pellet and in the cytoplasmic supernatant (Fig. 1 *a*, lanes *3* and *4*). The complete mitochondrial pellet was analyzed, whereas only ~1% of the other fractions were used on the blot to achieve equivalent RNA loading. Lanes containing RNA from uninfected A3.01 cells did not hybridize to the HIV-specific probe (Fig. 1 *a*, lane *1*). To assess the quality of mitochondrial and cytoplasmic fractions, the same Northern blot was also hybridized to probes specific to mitochondrial 12S rRNA and nuclear U1 snRNA. Fractions were significantly enriched for mitochondria because lane *3* showed high levels of 12S rRNA signal (Fig. 1 *a*, *12S panel*). Trace amounts of leakage from the nucleus during disruption were evident in mitochondria-enriched pellet because a weak signal for U1 snRNA was observed (Fig. 1 *a*, *U1 panel*, lanes *3* and *4*). Fig. 1 *b* represents the mitochondria-enriched pellet analyzed by electron microscopy. Contamination from cytoplasmic membrane structures were evident. These analyses suggested an association of HIV transcripts with mitochondrial fractions from infected cells. However, to strengthen the observation that a fraction of viral RNA was associated with mitochondria, we purified the mitochondria-enriched pellet further by Nycodenz gradient-density centrifugation. Mitochondria were separated from other membrane structures using the 12S rRNA profile as a marker. Results showed that HIV RNA was present in the first four fractions that contained light membrane structures. In addition, HIV RNA (5.5% of the HIV RNA present in the pellet) comigrated with mitochondrial-specific 12S RNA on Nycodenz gradients (coinciding peaks of HIV RNA and 12S rRNA in Fig. 1 *c*).

Viral RNA could be associated with mitochondria intracellularly or could be inside the organelle itself. To unequivocally demonstrate which of these occurred, viral RNA was visualized directly within thin sections of individual infected cells. In situ hybridization followed by colloidal gold antibodies to detect the biotin-labeled probe was used to ob-

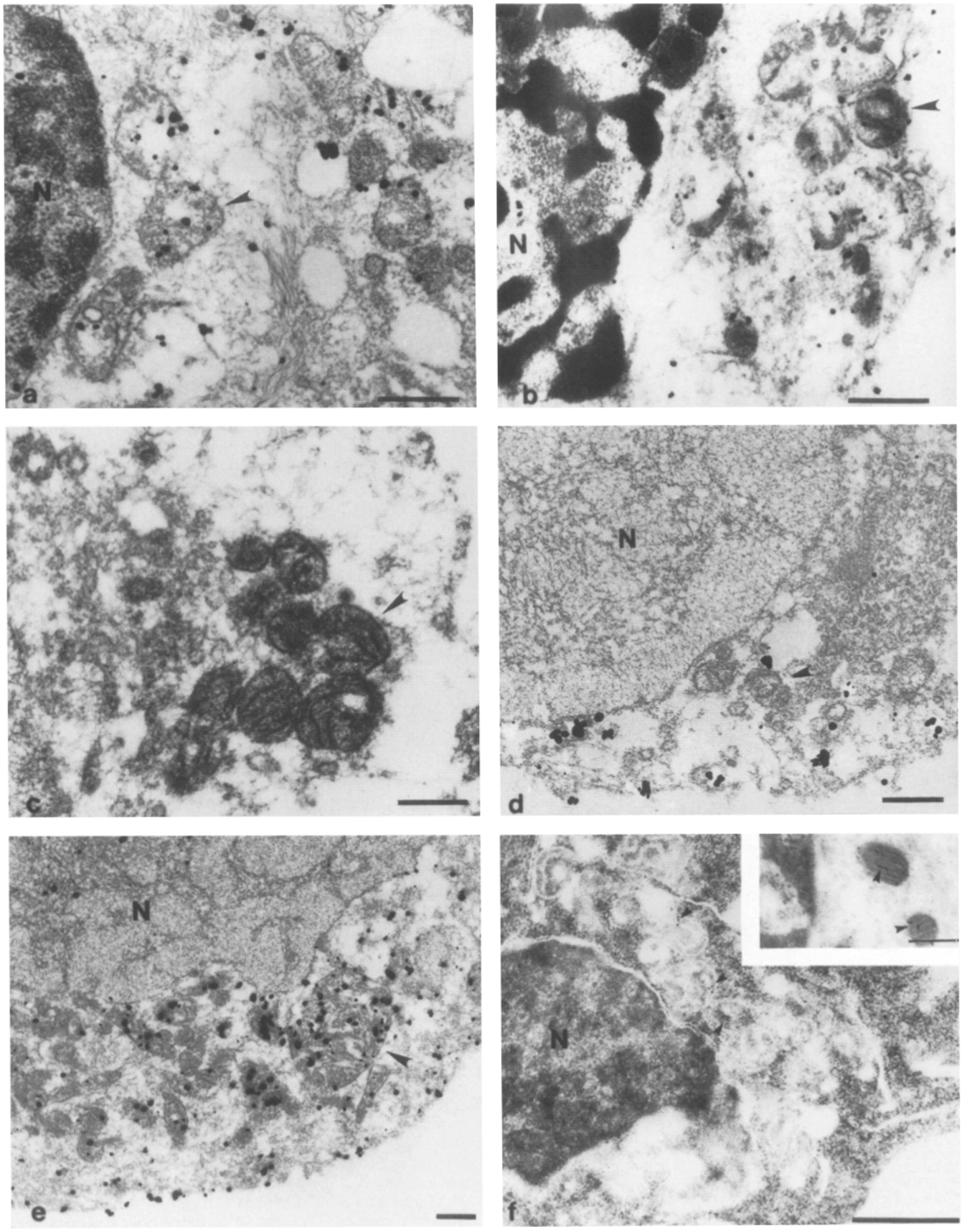

Figure 2. Detection and localization of HIV-1 RNA in infected cells using in situ hybridization and electron microscopy. (*a–e*) Viral RNA was detected by silver-enhanced gold (1) modified as described in Materials and Methods. (*a*) c8166 cells infected with HTLV-IIIB. (*b*) 8E5 cells. (*c*) Unstimulated ACH2 cells. (*d*) ACH2 cells TPA stimulated for 2 h. (*e*) ACH2 cells TPA stimulated for 6 h. Uninfected cells

serve localized viral RNA by electron microscopy (1). Infected and uninfected cells were inspected initially by light microscopy using silver to enhance the gold signal for light microscopic resolution and thereby verify the specificity of the hybridization only to infected cells. In thin sections, the HIV signal was immediately apparent in mitochondria (Fig. 2, *a* and *b*), as well as in the nucleus and cytoplasm. As a control, uninfected or latently infected cells (ACH2 cells) (Fig. 2 *c*) showed no signal. The in situ hybridization protocol was somewhat disruptive to cellular membranes; mitochondrial morphology in infected cells showed more effect of this than did the mitochondria of uninfected cells, perhaps indicating that the presence of viral RNA made their structure more fragile. To investigate this further, a protocol was developed which preserved the cell by standard ultrastructure approaches, and in situ hybridization was performed directly on the thin-sectioned material (5). In this way, the embedment preserved and protected the integrity of the organelle. Chemically biotinylated oligonucleotides were used as probes directly on thin sections (Fig. 2 *f*) since, because of their short length (30 nt), their penetration into the embedment was superior to nick-translated probes (26, 27). By this technique, the mitochondria and their cristae were visible by a negative stain (Fig. 2 *f*; membranes were only partially extracted), unlike Fig. 2, *a–e*. In addition to the morphologic identification of mitochondria, antibodies specific to a mitochondrial structural protein were used to confirm the specificity of the antibody for mitochondria (Fig. 2 *f*, *inset*).

These initial observations were then subjected to a quantitative analysis on the microscopic images. The distribution of silver grains within and outside the mitochondria was determined and expressed as grain density (percentage of silver grains/percentage of area). Results are presented in Table I. A positive signal was seen in HIV infected cells, and no signal was seen in the control uninfected cells. In addition to this, it was evident that mitochondria had concentrated levels of HIV RNA, despite the higher amounts of HIV RNA in the cytoplasm. The relative ratios of signal (density of silver grains) in mitochondria vs cytoplasm and nucleus ranged from 5.6 times (in chronically infected 8E5 cells) to 14.7 times (in acutely infected c8166 cells). The preferential concentration of HIV-1 RNA in the mitochondria was highly significant in both cell types ($P < 0.0001$). To ensure that this concentration in mitochondria was not an artifact of the protocol, the distribution in mitochondria of either viral proteins (*gag* p24) or of poly(A) RNA was assessed in the same manner after in situ hybridization. Viral antigen and poly(A) RNA were detected throughout the cell, but not in increased concentrations in mitochondria relative to the cytosol, in stark contrast to the observation on HIV RNA (Table I). The ratio of poly(A) RNA and p24 antigen distribution between the mitochondria and the cytoplasm and nucleus was ~1.2, and there was no preferential localization of either of these in mitochondria ($P > 0.5$). These results were consistent with an accumulation specifically of viral RNA within the mitochondria compared to other RNA or to viral specific products.

Table I. Quantitation of the Mitochondrial Localization of HIV-1 RNA in Acutely Infected or Chronically Infected Cells

Cell Type	Infection	Probed for	Density of mitochondrial grains	Density of grains outside mitochondria	Ratio
A3.01	Control	HIV	0.000	0.000	–
c8166	Acute	HIV	8.761	0.6248	14.7
8E5	Chronic	HIV	4.376	0.8563	5.63
8E5	Chronic	Poly A	1.278	0.9912	1.29
8E5	Chronic	p24	1.233	0.9959	1.24

The kinetics of viral RNA trafficking into mitochondria from sites of nuclear synthesis could be investigated using an inducible cell line and provided a time-dependent analysis of this mitochondrial import. ACH2 cells, at various times after TPA induction, were subjected to EM-in situ hybridization, and the data from the sections were analyzed as described previously. The viral RNA was seen to move rapidly into the mitochondria. Shortly after induction by this method, there was detectable viral RNA expression within the first hour, which continued to increase over the next 24 h. Eventually, the amount of viral RNA reached concentrations in the mitochondria that are seen in acute infections (Fig. 2, *d* and *e*; Table II). At all time points, a concomitant and highly significant ($P < 0.0001$) increase in the concentration of viral RNA in mitochondria was observed compared to the concentration in the cytoplasm and nucleus. These results, therefore, demonstrated rapid trafficking of viral RNA into mitochondria after activation of HIV-1 expression. This occurred as soon as viral RNA expression was detectable in the cytoplasm without any evidence of a time lag, or buildup in other cellular compartments during the time periods investigated.

Table II. Quantitation of the Mitochondrial Accumulation of HIV-1 RNA as a Function of Time after Induction

TPA stimulation time	Density of mitochondrial grains	Density of grains outside mitochondria	Ratio
h			
0	0.000	0.2222	0.00
1	3.762	0.6559	6.78
2	4.316	0.7523	7.00
4	3.661	0.6951	5.45
6	5.255	0.7558	7.29
12	7.843	0.8248	9.72
24	8.971	0.7297	12.26

treated in the same way did not show viral-specific staining; neither did infected cells when they were probed with non-HIV related sequences (not shown). The variation in sizes of mitochondria observed in the panels were caused by random sectioning of cells that resulted in longitudinal or transverse sections of mitochondria. (*f*) ACH2 cells TPA stimulated for 6 h were processed and viral RNA directly detected in thin sections as described in Materials and Methods. (*Inset*) Immunocytochemical analysis of uninfected A3.01 cells using mitochondrial-specific monoclonal antibody. The arrowheads indicate mitochondria in each panel. Bar, 5 μm. *N*, nucleus.

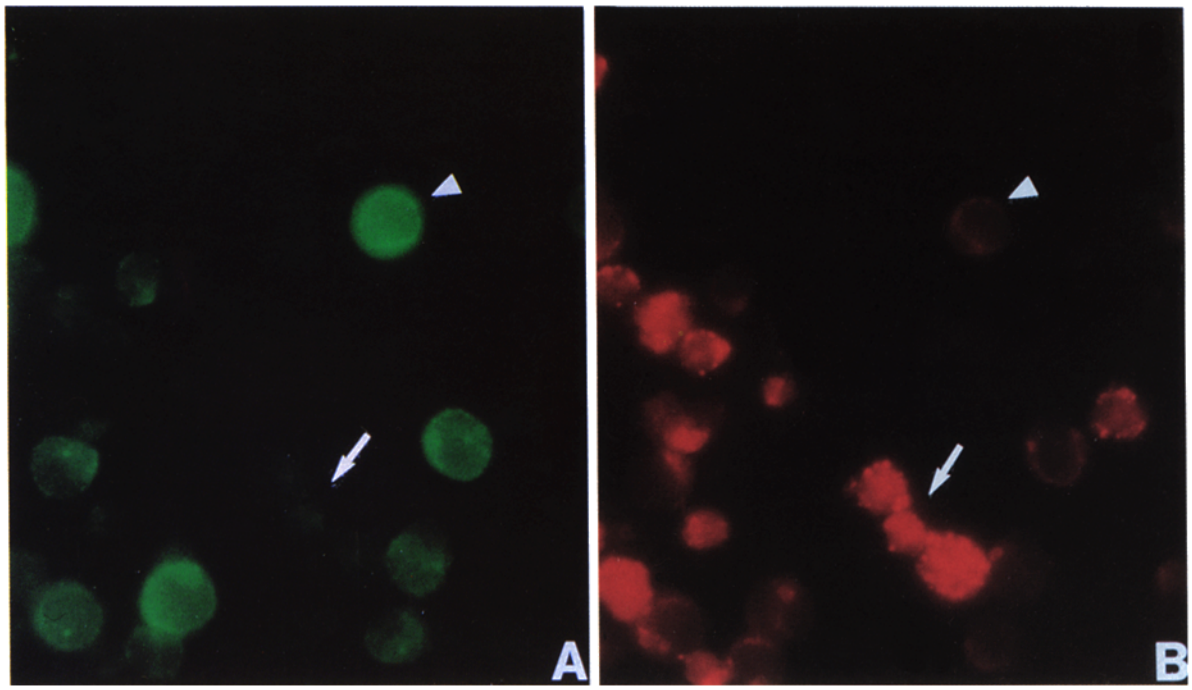

Figure 3. Analysis of HIV-1–positive cells double labeled for a mitochondrial antigen and viral RNA. ACH2 cells TPA stimulated for 6 h were washed and air-dried on slides. After fixation in 4% paraformaldehyde, the cells were washed, and HIV RNA was detected by in situ hybridization using biotinylated HIV probes and avidin-FITC as secondary reagent. The same cells were stained with mitochondrial-specific monoclonal antibody and goat anti–mouse IgG-TRITC was used as secondary reagent. (*A*) Field of ACH2 cells viewed for FITC fluorescence to detect HIV RNA. (*B*) Same field of cells viewed for TRITC fluorescence to detect cells with viable mitochondria. The arrowheads identify infected cells with high viral expression and diminished mitochondrial staining. The arrows identify a cluster of infected cells with weak viral expression and evident mitochondrial staining.

Viral Infection Affects Mitochondrial Viability

HIV RNA sequestration in mitochondria would be expected to be deleterious to mitochondrial function. To ascertain whether high levels of HIV RNA expression could affect mitochondrial integrity or function, individual TPA-stimulated ACH2 cells were analyzed simultaneously for the presence of viral RNA (Fig. 3 *A*) and a mitochondrial structural protein (Fig. 3 *B*) using dual-label fluorescence. The biotinylated probe was detected by fluorescein-avidin, whereas the mitochondria were detected by a rhodamine-conjugated antibody. Cells that showed high levels of viral RNA signal (*green*) were analyzed also for mitochondrial signal and had decreased mitochondrial-specific staining (*arrowheads*). Conversely, cells that show a strong signal for mitochondria (*red*) demonstrated a lack of HIV RNA signal (*arrows*). Hence, the mitochondrial antigen is either unavailable, degraded, or dispersed throughout the cytoplasm in cells acutely infected with HIV-1. These results are consistent with an inverse correlation between HIV RNA expression and structural integrity of mitochondria.

To verify that the structurally compromised mitochondria were also physiologically compromised, TPA-stimulated ACH2 cells and uninfected A3.01 cells were vitally stained with the fluorescent dye, rhodamine 123 (16), which is concentrated by viable mitochondria. Positive cells were quantitated by fluorescence intensity. The level of fluorescent labeling in ACH2 cells decreased from 88% of normal cells (at 0 h of TPA stimulation) to 32% (at 24 h), whereas staining of A3.01 T cells remained constant. These results are consistent with the hypothesis that increases in intracellular HIV expression impair mitochondrial functioning.

To test the effect of viral RNA expression on mitochondrial viability more rigorously, we assayed for mitochondrial dehydrogenases in TPA-stimulated ACH2 cells. The assay requires intact and functionally viable mitochondria to reduce the tetrazolium dye,3,(4,5-dimethylthiazol-2-yl)2,5 diphenyltetrazolium bromide (MTT; 3,18). Low levels of HIV RNA expression was detected with 1 h of TPA stimulation and levels of viral expression continued to increase with increasing time of TPA treatment. By 6 h of TPA treatment, ~80% of the cells in culture expressed viral RNA (data not shown) and HIV RNA was detected in mitochondria (Fig. 2 *e*). No substantial decrease in mitochondrial viability was observed (~90% of mitochondria were viable) during this period. However, over the next 20 h of TPA treatment, a decrease in mitochondrial enzyme activity was observed in ACH2 cells (Fig. 4, *open squares*) concomitant with increasing density of mitochondrial-associated viral RNA (Fig. 4, *open circles*) after induction with TPA. Uninfected T cells were assayed in parallel for mitochondrial viability after TPA treatment (Fig. 4, *open triangles*), and no decrease in mitochondrial viability was observed. These results further support the hypothesis that increases in intracellular HIV expression correlates with mitochondrial dysfunction.

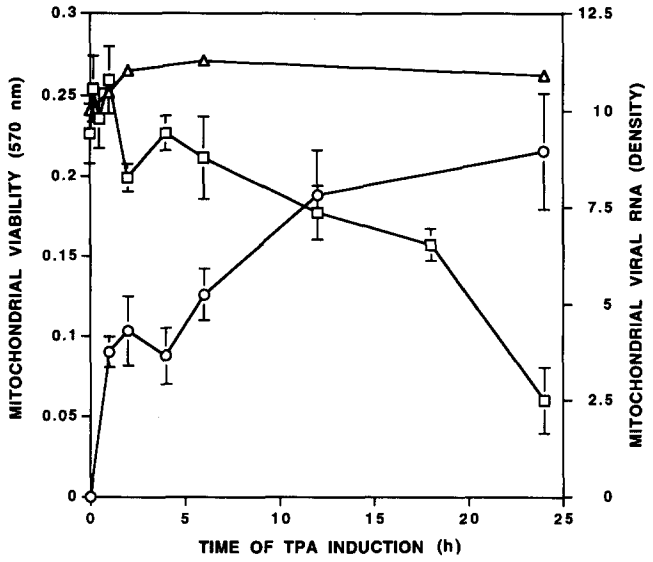

Figure 4. Determination of the functional activity of mitochondria in ACH2 cells after stimulation of viral expression. Mitochondrial enzymatic activity was measured in ACH2 cells (*open squares*) and in uninfected A3.01 cells (*open triangles*) stimulated by the phorbol ester, TPA, for various time periods. The density of viral RNA in mitochondria of ACH2 cells at each time was determined as described in Materials and Methods (*open circles*). Total active mitochondria in ACH2 cells was inversely related to levels of viral RNA accumulation in mitochondria (compare open squares to open circles). Mitochondrial activity of unstimulated ACH2 cells and TPA-induced uninfected A3.01 cells did not decrease during this period. The bars represent standard errors.

Possibly the loss of mitochondrial viability as a result of HIV RNA import correlates with the eventual death of the cell. The loss of mitochondrial viability within ACH2 cells induced for viral expression preceded cell death by ~24 h, as measured by dye exclusion. This suggested that accumulation of HIV-1 RNA in mitochondria may affect cell viability. It might be expected that cell lines propagating a chronic infection are viable because they have less virus in the mitochondria than acutely infected cells that ultimately undergo lysis because of a productive infection producing high levels of HIV RNA. Indeed, as demonstrated in Fig. 2 and Table I, quantitation of viral RNA by in situ hybridization revealed significantly less ($P < 0.005$) viral RNA in the mitochondria of cells from chronic cultures (8E5) compared to cells from acute cultures (c8166) (see Table I and Fig. 2, *a–c*). These results are consistent with the hypothesis that high concentrations of viral RNA could possibly disrupt the normal metabolism of mitochondria and lead to cell death.

In summary, five lines of evidence are presented here for support of an HIV-mitochondrial interaction: identification and copurification of HIV RNA within a mitochondrial fraction; a time-dependent concentration of HIV RNA within the mitochondria parallel viral RNA expression; disruption of mitochondrial integrity as a function of viral expression; loss of mitochondrial viability as a function of viral expression; and higher viral RNA concentrations in mitochondria of acutely infected cells compared to cells with a chronic infection. These data support the contention that viral RNA sequences may directly interfere with normal mitochondrial function.

The mechanism by which HIV RNA in mitochondria may be toxic is currently unknown. Possibly viral RNA affects mitochondrial function by competing with the import machinery for nucleic acids or proteins essential for mitochondrial viability. A mechanism for RNA import into mitochondria exists. A RNA component is essential for the functioning of an endoribonuclease (MRP complex), both of which are required for mitochondrial RNA processing in yeast and mammalian cells (2, 14, 24). Both the protein and its associated RNA are nuclear encoded, and they are subsequently imported into mitochondria, presumably as a complex. Recently, Li et al. have confirmed the existence of an RNA-mediated trafficking pathway for MRP-RNA in mouse cardiomyocytes using ultrastructural in situ hybridization and biochemical techniques (14). Using deletion mutants of the MRP-RNA gene, they have concluded that specific structural determinants within the MRP-RNA were recognized by components responsible for mitochondrial import.

The HIV RNA found in the mitochondria may be imported in two possible ways: either a viral factor(s) or a cellular factor(s) may transport the RNA in a complex. A candidate for the protein component of a transport complex is Rev, which is known to redistribute HIV RNA between the nucleus and the cytoplasm. Preliminary studies suggest that Rev did not interact with human MRP-RNA gene transcripts, nor was it found in higher levels in mitochondria, and thus, it may not be involved in mitochondrial transport of HIV RNA (data not shown). The alternative possibility is that cellular factor(s) may bind to viral sequences, such as the Rev-responsive element, and be involved in the transport mechanism. A comparison between HIV RNA and human MRP-RNA did not show sequence homology with the putative import sequences (14), but did reveal a region of 27 nt with 67% homology between the end of the viral Rev-responsive element and the end of the MRP-RNA. Currently, work is directed toward determining if this region or additional sequences within HIV RNA are responsible for a possible "mistaken identity" that may target the HIV RNA to mitochondria. Further work will confirm and define the specificity of this interaction, and will assist in characterization of the components involved in the nucleo-mitochondrial pathway.

We thank Drs. Michael Green, Harriet Robinson, Gregory Viglianti, and Trudy Morrison for their critical review of this manuscript, Chris Powers for her assistance in electron microscope studies, and James Hebert with the statistical programs. This work was supported by a National Institutes of Health (NIH) grant (HL-42257) and an NIH contract (HB-67022).

Received for publication 7 January 1994, and in revised form 13 June 1994.

References

1. Bassell, G. S., and R. H. Singer. 1992. Ultrastructural in situ hybridization using immuno-gold. *In* Immuno-gold Electron Microscopy in Virus Diagnosis and Research. A. Hyatt and B. Eaton, editors. CRC Press, Boca Raton, FL. pp. 377–409.
2. Chang, D. D., and D. A. Clayton. 1987. A mammalian mitochondrial RNA processing activity contains nucleus-encoded RNA. *Science (Wash. DC).* 235:1178–1184.
3. Denizot, F., and R. Lang. 1986. Rapid colorimetric assay for cell growth and survival: modifications to the tetrazolium dye procedure giving improved sensitivity and reliability. *J. Immunol. Methods.* 89:271–277.
4. Di Franco, A., M. Russo, and G. P. Martelli. 1984. Ultrastructure and origin of cytoplasmic multivesicular bodies induced by carnation Italian ringspot virus. *J. Gen. Virol.* 65:1233–1237.

5. Escaig-Haye, F., V. Grigoriev, G. Peranzi, P. Lestienne, and J.-G. Fournier. 1991. Analysis of human mitochondrial transcripts using electron microscopic in situ hybridization. *J. Cell. Sci.* 100:851–862.
6. Folks, T. M., D. Powell, M. Lightefoot, S. Koenig, A. S. Fauci, S. Benn, A. Rabson, D. Daugherty, H. E. Gendelman, M. D. Hoggan, et al. 1986. Biological and biochemical characterization of a cloned Leu-3⁻ cell surviving infection with the acquired immune deficiency syndrome retrovirus. *J. Exp. Med.* 164:280–290.
7. Garzon, S., H. Strykowski, and G. Charpentier. 1990. Implication of mitochondria in the replication of Nodamura virus in larvae of the *Lepidopetra, Gallerai mellonella* (L.) and suckling mice. *Arch. Virol.* 113: 165–176.
8. Ho, D. D., T. Moudgil, and M. Alam. 1989. Quantitation of human immunodeficiency virus type 1 in the blood of infected persons. *N. Engl. J. Med.* 321:1621–1625.
9. Hoxie, J. A., J. D. Alpers, J. L. Rackowski, K. Huebner, B. S. Haggarty, A. J. Cedarbaum, and J. C. Reed. 1986. Alterations in T4(CD4) protein synthesis and mRNA synthesis in cells infected with HIV. *Science (Wash. DC).* 234:1123–1127.
10. Kara, J., O. Mach, and H. Cerna. 1971. Replication of Rous sarcoma virus and the biosynthesis of the oncogenic subviral ribonucleoprotein particles (virosomes) in the mitochondria isolated from Rous sarcoma tissue. *Biochem. Biophys. Res. Commun.* 44:162–170.
11. Koga, Y., M. Sasaki, H. Yoshida, M. Oh-Tsu, G. Kimura, and K. Nomoto. 1991. Disturbance of nuclear transport of proteins in CD4⁺ cells expressing gp160 of human immunodeficiency virus. *J. Virol.* 65:5609–5612.
12. Laurent-Crawford, A. G., B. Krust, S. Muller, Y. Rivire, M. A. Rey-Cuille, J. M. Bechet, L. Montagnier, and A. G. Hovanessian. 1991. The cytopathic effect of HIV is associated with apoptosis. *Virology.* 189: 695–714.
13. Lawrence, J. B., L. M. Marselle, K. S. Byron, C. V. Johnson, J. L. Sullivan, and R. H. Singer. 1990. Subcellular localization of low-abundance human immunodeficiency virus nucleic acid sequences visualized by fluorescence in situ hybridization. *Proc. Natl. Acad. Sci. USA.* 87:5420–5424.
14. Li, K., C. S. Smagula, W. J. Parsons, J. A. Richardson, M. Gonzalez, H. K. Hagler, and R. S. Williams. 1994. Subcellular partitioning of MRP RNA assessed by ultrastructural and biochemical analysis. *J. Cell Biol.* 124:871–882.
15. Lifson, J. D., M. B. Feinberg, G. R. Reyes, L. Rabin, B. Banapour, S. Chakrabarti, B. Moss, F. Wong-Staal, K. S. Steimer, and E. G. Engelman. 1986. Induction of CD4-dependent cell fusion by the HTLV-III/LAV envelope glycoprotein. *Nature (Lond.).* 323:725–728.
16. Lynch, R. M., K. E. Fogarty, and F. S. Fay. 1991. Modulation of hexokinase association with mitochondria analyzed with quantitative three-dimensional confocal microscopy. *J. Cell Biol.* 112:385–395.
17. Matsumaya, T., N. Kobayashi, and N. Yamamoto. 1991. Cytokines and HIV-infection: is AIDS a tumor necrosis factor disease? *AIDS.* 5:1405–1417.
18. Mosmann, T. 1983. Rapid colorimetric assay for cellular growth and survival: application to proliferation and cytotoxicity assays. *J. Immunol. Methods.* 65:55–63.
19. Pang, S., Y. Koyanagi, S. Miles, C. Wiley, H. V. Vinters, and I. S. Y. Chen. 1990. High levels of unintegrated HIV-1 DNA in brain tissue of AIDS dementia patients. *Nature (Lond.).* 343:85–89.
20. Pantaleo, G., C. Graziosi, J. F. Demarest, L. Butini, M. Montroni, C. H. Fox, J. M. Orenstein, D. P. Kotler, and A. S. Fauci. 1993. HIV infection is active and progressive in lymphoid tissue during the clinically latent stage of disease. *Nature (Lond.).* 362:355–358.
21. Pauza, C. D., J. E. Galinde, and D. D. Richman. 1990. Reinfection results in accumulation of unintegrated viral DNA in cytopathic and persistent human immunodeficiency virus type 1 infection of CEM cells. *J. Exp. Med.* 172:1035–1042.
22. Rosenberg, Z. F., and A. S. Fauci. 1990. Immunopathogenic mechanisms of HIV infection: cytokine induction of HIV expression. *Immunol. Today.* 11:176–180.
23. Saag, M. S., M. J. Crain, W. D. Decker, S. Campbell-Hill, S. Robinson, W. E. Brown, M. Leuther, R. J. Whitley, B. H. Hahn, and G. M. Shaw. 1991. High level viremia in adult and children infected with human immunodeficiency virus: relation to disease stage and CD4⁺ lymphocyte levels. *J. Infect. Dis.* 164:72–80.
24. Schmitt, M. E., and D. A. Clayton. 1992. Yeast site-specific ribonucleoprotein endoribonuclease MRP contains an RNA component homologous to mammalian RNAse MRP RNA and essential for cell viability. *Genes & Dev.* 6:1975–1985.
25. Shaw, G. M., B. H. Hahn, S. K. Arya, J. E. Groopman, R. C. Gallo, and F. Wong-Staal. 1984. Molecular characterization of human T-cell leukemia (lymphotropic) virus type III in the acquired immune deficiency syndrome. *Science (Wash. DC).* 226:1165–1171.
26. Singer, R. H., K. S. Byron, J. B. Lawrence, and J. L. Sullivan. 1989. Detection of HIV-1 infected cells from patients using nonisotopic in situ hybridization. *Blood.* 74:2295–2301.
27. Singer, R. H., J. B. Lawrence, R. Bashir, K. S. Byron, and J. L. Sullivan. 1990. Diagnostic applications of nonisotopic in situ hybridization of HIV or EBV nucleic acids. *In* Modern Pathology of AIDS and Other Retroviral Infections. P. Racz, A. T. Haase, and J. C. Gluckman, editors. Karger, Basel, pp. 29–41.
28. Sodroski, J., W. C. Goh, C. Rosen, A. Dayton, E. Terwilliger, and W. A. Haseltine. 1986. Role of the HTLV-III/LAV envelope in syncytium formation and cytopathicity. *Nature (Lond.).* 322:470–474.
29. Somasundaran, M., and H. L. Robinson. 1987. A major mechanism of human immunodeficiency virus-induced cell killing does not involve cell fusion. *J. Virol.* 61:3114–3119.
30. Somasundaran, M., and H. L. Robinson. 1988. Unexpectedly high levels of HIV-1 RNA and protein synthesis in a cytocidal infection. *Science (Wash. DC).* 242:1554–1557.
31. Terai, C., R. S. Kornbluth, C. D. Pauza, D. D. Richman, and D. A. Carson. 1991. J. Clin. Invest. Apoptosis as a mechanism of cell death in cultured T lymphoblasts acutely infected with HIV-1. 87:1710–1715.
32. Topper, D. P., R. A. Van Etten, and D. A. Clayton. 1983. Isolation of mammalian mitochondrial DNA and RNA and cloning of the mitochondrial genome. *Methods Enzymol.* 97:426–435.
33. Xie, W., and L. I. Rothblum. 1991. Rapid, small-scale RNA isolation from tissue culture cells. *Biofeedback.* 11:335–337.